

## SYNTHESIS, CHARACTERIZATION AND THERMAL BEHAVIOUR OF SOLID-STATE COMPOUNDS OF YTTRIUM AND LANTHANIDE BENZOATES

J. R. Locatelli<sup>1</sup>, E. C. Rodrigues<sup>2</sup>, A. B. Siqueira<sup>2</sup>, E. Y. Ionashiro<sup>2</sup>, G. Bannach<sup>2</sup> and M. Ionashiro<sup>2\*</sup>

<sup>1</sup> Academia da Força Aérea, AFA. Estrada de Aguai; s/n, CEP 13630-000 Pirassununga, SP, Brazil

<sup>2</sup> Instituto de Química, UNESP, C. P. 355, CEP 14801 – 970 Araraquara, SP, Brazil

Solid-state  $\text{Ln}(\text{Bz})_3 \cdot \text{H}_2\text{O}$  compounds where Ln stands for trivalent yttrium or lanthanides and Bz is benzoate have been synthesized. Simultaneous thermogravimetry-differential thermal analysis (TG-DTA), X-ray powder diffractometry, infrared spectroscopy and chemical analysis were used to characterize and to study the thermal behaviour of these compounds. The results led to information about the composition, dehydration, thermal stability and thermal decomposition of the isolated compounds.

**Keywords:** benzoate, lanthanides, thermal behaviour

### Introduction

Benzoic acid and some of its derivatives are used as preservative, catalyst polymer precursor, in pharmaceutical industries, etc. A survey of the literature shows that the complexes of rare earth and d-block elements with benzoic acids and some of their derivatives have been investigated in aqueous solution and in solid state.

The papers report on the thermodynamics of complexation of lanthanides by some benzoic acid derivatives [1] in solution, on the spectroscopic study of trivalent lanthanides with several carboxylic acids including benzoic acid [2], the influence of pH, surfactant and synergic agent on the luminescent properties of terbium chelates with benzoic acid derivatives [3]. The thermodynamic of complexation of lanthanides by benzoic and isophthalic acids is dealt in [4], while the synthesis, crystal structure, photophysical and magnetic properties of dimeric and polymeric lanthanide complexes with benzoic acid and its derivatives were described in [5].

Among the solid state properties the thermal stability and thermal decomposition of thorium salts with several organic acids, including 4-methoxybenzoic acid is reported in [6], as well as benzoic and *m*-hydroxybenzoic acids in [7]; the thermal decomposition of nickel benzoate and of the nickel salt of cyclohexane carboxylic acid in [8]; the thermal and spectral behaviour on solid compounds of benzoates and its methoxy derivates with rare earth elements in

[9–12, 14–17]. The vibrational and electronic spectroscopic study of lanthanides and effect of sodium on the aromatic system of benzoic acid is surveyed in [13, 16]; the reaction of bivalent copper, cobalt and nickel with 3-hydroxy-4-methoxy and 3-methoxy-4-hydroxybenzoic acids and a structure for these compounds has been proposed on the basis of spectroscopic and thermogravimetric data [18]; the thermal decomposition of thorium salts of benzoic and 4-methoxybenzoic acids in air atmosphere [19]; the thermal and spectral behaviour on solid compounds of 5-chloro-2-methoxybenzoate with rare earth and d-block elements [20–23]; the synthesis and characterization of 2,3-dimethoxybenzoates of heavy lanthanides and yttrium [24]; the thermal studies on solid compounds of phenyl substituted derivates of benzylidenepruvates with several metal ions [25, 26]; the spectral and magnetic studies of 2-chloro-5-nitrobenzoates of rare earth elements [27]; thermal behaviour of solid state 2-methoxybenzoates, 3-methoxybenzoates, 4-methoxybenzoates of some bivalent transition metal ions [28–30]; and thermal behaviour of solid state 4-methoxybenzoates of trivalent lanthanides [31, 32].

In the present study benzoates of Y(III) and trivalent lanthanides, except Pm, were synthesized. The compounds were investigated by means of infrared spectroscopy, X-ray powder diffractometry, simultaneous thermogravimetry-differential thermal analysis (TG-DTA) and other analytical methods.

\* Author for correspondence: massaoi@iq.unesp.br

## Experimental

The benzoic acid (HBz) with 99.9% purity was obtained from Merck. Aqueous solution of Na-Bz (0.1 mol L<sup>-1</sup>) was prepared by neutralization aqueous HBz suspension with 0.1 mol L<sup>-1</sup> sodium hydroxide solution.

Yttrium(III) and lanthanide(III) chlorides were prepared from the corresponding metal oxides (except for cerium) by treatment with concentrated hydrochloric acid. The resulting solutions were evaporated to near dryness, the residues were redissolved in distilled water and the solutions have been again evaporated to near dryness to eliminate the excess of hydrochloric acid. Then, the residues were again dissolved in distilled water, transferred to a volumetric flask and diluted in order to obtain ca. 0.10 M solutions, whose pH were adjusted to 5.0 by adding diluted sodium hydroxide or hydrochloric acid solutions. Ca. 0.10 M aqueous solution of cerium(III) nitrate was made by direct weighing of the solid salt according to [33].

The solid-state compounds were prepared by slow addition of the aqueous solution of NaBz with continuous stirring to the respective metal chloride or nitrate solutions, until total precipitation of the metal ions. The precipitates were washed with distilled water to eliminate the chloride (or nitrate ions), then filtered through and dried on Whatman n° 42 filter paper, and kept in a desiccator over anhydrous calcium chloride, under reduced pressure to obtain a constant mass.

In the solid state compounds hydration water, ligand and metal ion content was determined from TG curves. The metal ions were also determined by

complexometric titrations with standard EDTA solution using xylenol orange as indicator [34].

X-ray powder patterns were obtained by using a Siemens D-5000 X-ray diffractometer with CuK $\alpha$  radiation ( $\lambda=1.541\text{ \AA}$ ) and under 40 kV and 20 mA settings. Infrared spectra for NaBz (sodium salt) as well as for its metal-ion compounds were recorded on a Nicolet model Impact 400 FTIR instrument in the 4000–400 cm<sup>-1</sup> range. The solid samples were pressed into KBr pellets.

Simultaneous TG-DTA curves were obtained applying TA SDT 2960 thermoanalytical unit (TA Instruments, USA) with air purging (flow rate: 100 mL min<sup>-1</sup>) and at a heating rate of 20°C min<sup>-1</sup>. The initial sample mass was about 7 mg and platinum crucibles were used for the TG-DTA experiments.

### Computational strategy

To calculation of the theoretical infrared spectrum of lanthanum benzoate, it is necessary to evaluate the structure and wave function computed by the ab initio SCF Hartree–Fock–Roothan method [35] using a split valence (LanL2DZ) basis set [36–39]. The performed molecular calculations in this work were done by using the Gaussian 98 routine [40] and the hardware used was IBM power 3. The crystal geometry of lanthanum benzoate is unknown. The geometrical optimization was carried out without any constraints. The benzoate molecule contains rings with conformational flexibility and all variables were optimized. The optimization proceeded more uniformly when all variables were optimized.

**Table 1** Analytical data for Ln(Bz)<sub>3</sub>·nH<sub>2</sub>O

Compound	Water/%		Ligand lost/%		Metal oxide/%			Residue
	Calcd.	TG	Calcd.	TG	Calcd.	TG	EDTA	
La(Bz) <sub>3</sub> ·2H <sub>2</sub> O	6.70	6.73	63.04	63.48	30.26	29.79	30.35	La <sub>2</sub> O <sub>3</sub>
Ce(Bz) <sub>3</sub> ·2H <sub>2</sub> O	6.68	6.70	61.42	61.30	31.90	32.00	31.76	CeO <sub>2</sub>
Pr(Bz) <sub>3</sub> ·2H <sub>2</sub> O	6.67	6.84	61.82	61.76	31.51	31.40	31.74	Pr <sub>6</sub> O <sub>11</sub>
Nd(Bz) <sub>3</sub> ·2.5H <sub>2</sub> O	8.15	7.90	61.41	61.55	30.44	30.55	30.03	Nd <sub>2</sub> O <sub>3</sub>
Sm(Bz) <sub>3</sub> ·2H <sub>2</sub> O	6.56	6.65	61.73	61.49	31.71	31.86	31.62	Sm <sub>2</sub> O <sub>3</sub>
Eu(Bz) <sub>3</sub> ·1.5H <sub>2</sub> O	4.98	5.15	62.57	62.50	32.45	32.35	32.21	Eu <sub>2</sub> O <sub>3</sub>
Gd(Bz) <sub>3</sub> ·1.5H <sub>2</sub> O	4.94	5.03	61.96	61.78	33.10	33.19	32.88	Gd <sub>2</sub> O <sub>3</sub>
Tb(Bz) <sub>3</sub> ·H <sub>2</sub> O	3.34	3.40	62.06	62.14	34.60	34.46	34.60	Tb <sub>4</sub> O <sub>7</sub>
Dy(Bz) <sub>3</sub> ·0.5H <sub>2</sub> O	1.68	1.72	63.45	63.28	34.87	35.00	34.55	Dy <sub>2</sub> O <sub>3</sub>
Ho(Bz) <sub>3</sub>	–	–	64.24	64.18	35.76	35.82	35.57	Ho <sub>2</sub> O <sub>3</sub>
Er(Bz) <sub>3</sub>	–	–	63.96	63.83	36.04	36.17	36.01	Er <sub>2</sub> O <sub>3</sub>
Tm(Bz) <sub>3</sub>	–	–	63.75	63.65	36.24	36.35	36.58	Tm <sub>2</sub> O <sub>3</sub>
Yb(Bz) <sub>3</sub>	–	–	63.27	63.34	36.73	36.66	36.85	Yb <sub>2</sub> O <sub>3</sub>
Lu(Bz) <sub>3</sub>	–	–	63.10	62.86	36.90	37.14	36.71	Lu <sub>2</sub> O <sub>3</sub>
Y(Bz) <sub>3</sub>	–	–	75.03	74.99	24.97	25.01	24.90	Y <sub>2</sub> O <sub>3</sub>

Ln=Yttrium(III), or trivalent lanthanides; Bz=benzoate

## Results and discussion

The analytical and thermoanalytical (TG) data are shown in Table 1. These results establish the stoichiometry of these compounds, which are in agreement with the  $\text{Ln}(\text{Bz})_3 \cdot n\text{H}_2\text{O}$  general formula, where Ln represents trivalent yttrium and lanthanides, Bz is benzoate and  $n=2.5$  (Nd), 2 (La, Ce, Pr, Sm), 1.5 (Eu, Gd), 1 (Tb), 0.5 (Dy) and 0 (Ho to Lu and Y).

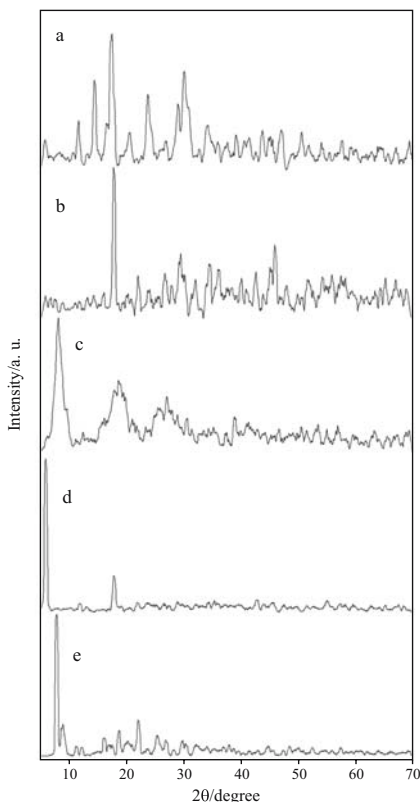
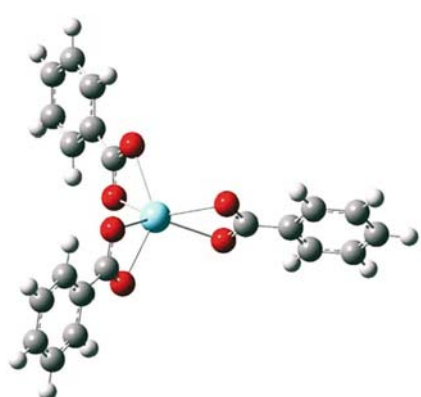


**Fig. 1** X-ray powder diffraction patterns of: a –  $\text{La}(\text{Bz})_3 \cdot 2\text{H}_2\text{O}$ ; b –  $\text{Ce}(\text{Bz})_3 \cdot 2\text{H}_2\text{O}$ ; c –  $\text{Dy}(\text{Bz})_3 \cdot 0.5\text{H}_2\text{O}$ ; d –  $\text{Pr}(\text{Bz})_3 \cdot 2\text{H}_2\text{O}$  as representative of the Nd to Tb compounds and e –  $\text{Ho}(\text{Bz})_3$  as representative of Er to Lu and Y compounds ( $\text{Bz}$ =benzoate)



The X-ray diffraction powder patterns (Fig. 1) show that all the compounds have a crystalline structure, except lanthanum(III), cerium(III) and dysprosium(III) compounds, evidencing the formation of two isomorphous series: being the praseodymium(III) to terbium(III) compounds the first one and the holmium(III) to lutetium(III) and yttrium(III) compounds the other series.

Infrared spectroscopic data on sodium benzoate and its compounds and with the metal ions considered in this work are shown in Table 2. The investigation was focused mainly in the  $1700\text{--}1400\text{ cm}^{-1}$  range because this region is potentially the most informative to assign the coordination sites.

The anti-symmetrical and symmetrical vibration bands of carboxylate anions appeared in the spectra of yttrium(III) and lanthanide(III) compounds within the ranges  $\nu_{\text{as}}(\text{COO}^-)=1539\text{--}1522\text{ cm}^{-1}$ ,  $\nu_s(\text{COO}^-)=1427\text{--}1416\text{ cm}^{-1}$ ; for the sodium benzoate at  $\nu_{\text{as}}(\text{COO}^-)=1551\text{ cm}^{-1}$  and  $\nu_s(\text{COO}^-)=1414\text{ cm}^{-1}$  frequencies.

Analysis of the  $\nu_{\text{as}}$  and  $\nu_s(\text{COO}^-)$  bands shows that the lanthanides(III) are linked to the carboxylic group by a bidentate bond with an incomplete equalization of bond lengths in the carboxylate anion; this is in agreement with the literature data [41, 42].

The theoretical infrared spectrum of  $\text{La}(\text{Bz})_3 \cdot 3\text{H}_2\text{O}$  was calculated by using a harmonic field [43] and the obtained frequencies were not scaled. The geometry optimization was computed by the optimized Berny algorithm [44]. The obtained geometry from calculations is presented in Fig. 2 and Table 3.

The theoretical infrared spectrum (electronic state  ${}^1\text{A}$ ) was obtained with frequency values ( $\text{cm}^{-1}$ ), relative intensities, assignments and description of vibrational modes.

A comparative analysis between the experimental and theoretical spectrum shows the following conclusions: (a) the first assignment shows a strong contribution at  $1535\text{ cm}^{-1}$  suggesting a  $\nu_{\text{asym}}(\text{COO}^-)$  as-

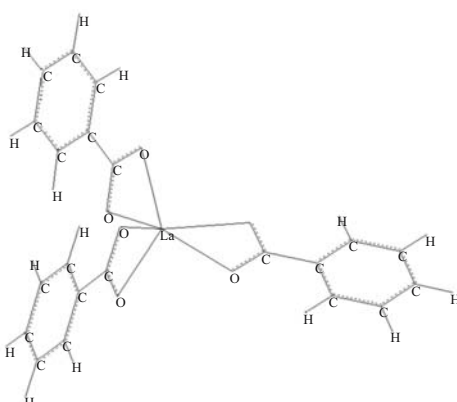


**Fig. 2** Proposed structure 3D of solid-state anhydrous compound lanthanum(III) with benzoate (optimized using Hartree–Fock–Roothan method, LanL<sub>2</sub>DZ basis set of Gaussian 98)

**Table 2** Spectroscopic data for sodium benzoate and compounds with lanthanides(III) and yttrium(III)

Compounds	$\nu_{(O-H)}$ H <sub>2</sub> O	$\nu_s(COO^-)$	$\nu_{as}(COO^-)$	$\Delta(\nu_s(COO^-) - \nu_{as}(COO^-))$
NaBz	—	1414 s	1551 s	137
La(Bz) <sub>3</sub> ·2H <sub>2</sub> O	3449	1425 s	1535 s	110
Ce(Bz) <sub>3</sub> ·2H <sub>2</sub> O	3454	1427 s	1533 s	106
Pr(Bz) <sub>3</sub> ·2H <sub>2</sub> O	3448	1427 s	1533 s	106
Nd(Bz) <sub>3</sub> ·2.5H <sub>2</sub> O	3438	1417 s	1531 s	114
Sm(Bz) <sub>3</sub> ·2H <sub>2</sub> O	3462	1423 s	1533 s	110
Eu(Bz) <sub>3</sub> ·1.5H <sub>2</sub> O	3440	1423 s	1537 s	114
Gd(Bz) <sub>3</sub> ·1.5H <sub>2</sub> O	3442	1423 s	1539 s	116
Tb(Bz) <sub>3</sub> ·H <sub>2</sub> O	3452	1419 s	1539 s	120
Dy(Bz) <sub>3</sub> ·0.5H <sub>2</sub> O	3450	1418 s	1531 s	113
Ho(Bz) <sub>3</sub>	—	1416 s	1522 s	106
Er(Bz) <sub>3</sub>	—	1418 s	1524 s	106
Tm(Bz) <sub>3</sub>	—	1418 s	1526 s	108
Yb(Bz) <sub>3</sub>	—	1418 s	1526 s	108
Lu(Bz) <sub>3</sub>	—	1419 s	1523 s	104
Y(Bz) <sub>3</sub>	—	1418 s	1526 s	108

s=strong, Bz=benzoate; s strong; b broad;  $\nu_{as(O-H)}$ =hydroxyl group stretching frequency;  $\nu_s(COO^-)$  and  $\nu_{as}(COO^-)$ =symmetrical and anti-symmetrical vibrations of the COO<sup>-</sup> group respectively

gment, while the theoretical results show the corresponding peak at 1531 cm<sup>-1</sup> with 0.3% discrepancies; (b) the second assignment shows a strong contribution at 1425 cm<sup>-1</sup> suggesting a  $\nu_{sym}(COO^-)$  assignment, while the theoretical results show the corresponding peak at 1386 cm<sup>-1</sup> with 2.7% discrepancies; (c) the third assignment shows both experimental and theoretical  $\Delta\nu$  values ( $\nu_{asym}(COO^-) - \nu_{sym}(COO^-)$ ) are near the sodium benzoate  $\Delta\nu$  value ( $\Delta\nu_{Na}=127$ ;  $\Delta\nu_{exp}=103$ ;  $\Delta\nu_{Theor}=140$ ) reinforcing the suggestion that compounds considered in this work have a covalent bidentate bond.

The simultaneous TG–DTA curves of the compounds are shown in Fig. 2. These curves exhibit mass loss in steps and thermal events corresponding to these losses or due to physical phenomenon. Three thermal steps are observed for these compounds. At first, similar TG–DTA profiles can be observed for La(III), Nd(III), Sm(III) and Eu(III) compounds, where the thermal decomposition occurs in four steps. A close similarity was observed for the Ce(III), Pr(III), Gd(III), Tb(III) and Dy(III) compounds, where the thermal decomposition occurs in the three steps. On the contrary, Ho(III) to Lu(III) and Y(III) compounds display another set of very similar TG–DTA profiles and the thermal decomposition occurs in two steps.

Thus the features of each of these compounds are discussed on the base of their similar thermal profiles.

### Lanthanum(III), Neodymium(III), Samarium(III) and Europium III) compounds

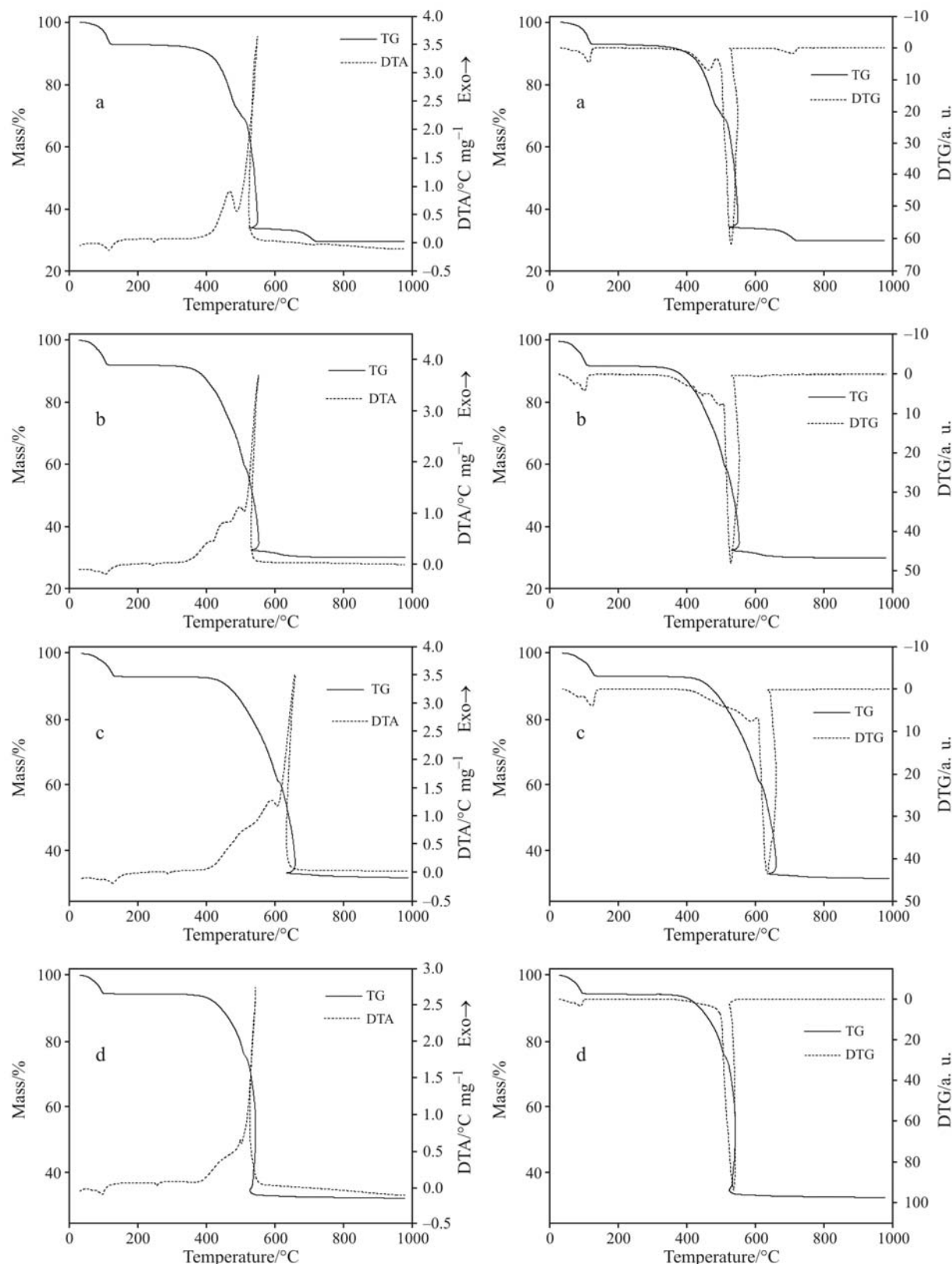
The TG–DTA curves of the lanthanum(III) and europium(III) as representative of these compounds are shown in Fig. 3. The first mass loss up to 125°C (La), 120°C (Nd) and 110°C (Sm, Eu) with the corresponding endothermic peaks at 115°C (La), 110°C (Nd), 105°C (Sm) and 100°C (Eu) is due to the release of 2.5H<sub>2</sub>O (Nd), 2H<sub>2</sub>O (La, Sm) and 1.5H<sub>2</sub>O (Eu) moles of water.

After their dehydration the anhydrous compounds are stable up to 320°C and the endothermic peaks at 255°C (La), 250°C (Nd, Eu) and 320°C (Sm) are attributed to the reversible crystalline phase transition confirmed by X-ray powder diffraction and TG–DTA analysis.

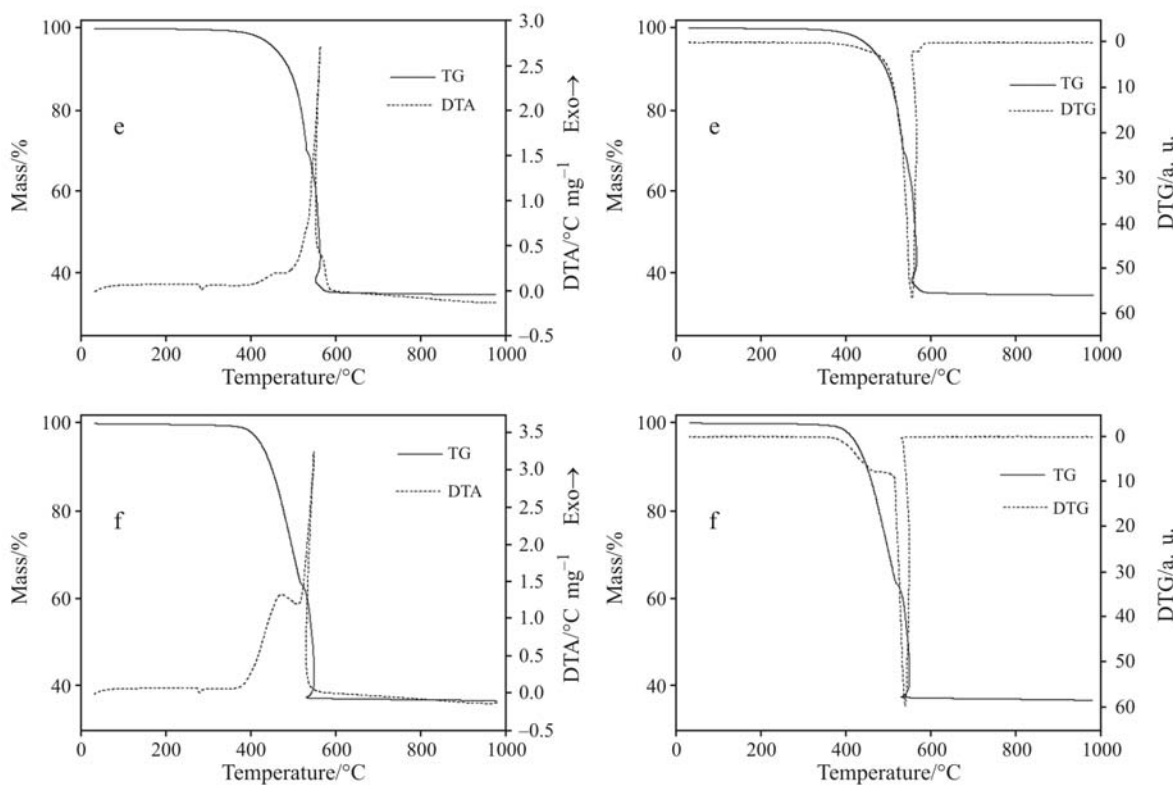
**Table 3** Theoretical geometries parameters of La(Bz)<sub>3</sub> compound

<i>d</i>	La – O <sub>coo<sup>-</sup></sub>	2.54 Å
<i>d</i>	C <sub>coo<sup>-</sup></sub> – O <sub>coo<sup>-</sup></sub>	1.29 Å
<i>d</i>	C <sub>coo<sup>-</sup></sub> – C <sub>ring</sub>	1.47 Å
<i>d</i>	C <sub>ring</sub> – C <sub>ring</sub>	1.39 Å
<i>d</i>	C <sub>ring</sub> – H <sub>ring</sub>	1.07 Å
<	O <sub>coo<sup>-</sup></sub> – C <sub>coo<sup>-</sup></sub> – O <sub>coo<sup>-</sup></sub>	116.76°
<	O <sub>coo<sup>-</sup></sub> – La – O <sub>coo<sup>-</sup></sub>	64.34°
<	C <sub>ring</sub> – C <sub>ring</sub> – C <sub>ring</sub>	119.84°

Key: La=lanthanum; Bz=benzoate; *d*=atoms distance; <=atoms angle; COO<sup>-</sup>=carboxylate; ring=benzene ring



**Fig. 3** TG-DTA and TG/DTG curves of: a –  $\text{La}(\text{Bz})_3 \cdot 2\text{H}_2\text{O}$  (6.943 mg); b –  $\text{Eu}(\text{Bz})_3 \cdot 1.5\text{H}_2\text{O}$  (6.966 mg); c –  $\text{Ce}(\text{Bz})_3 \cdot 2\text{H}_2\text{O}$  (6.964 mg); d –  $\text{Gd}(\text{Bz})_3 \cdot 1.5\text{H}_2\text{O}$  (6.929 mg); e –  $\text{Ho}(\text{Bz})_3$  (7.029 mg) and f –  $\text{Yb}(\text{Bz})_3$  (7.244 mg) ( $\text{Bz}$ =benzoate)

**Fig. 3 (continued)**

The thermal decomposition of the anhydrous compounds occurs in three steps. The first two corresponding to exothermic peaks, attributed to the oxidation of the organic matter. The TG–DTA profiles of the second step show that the oxidation of organic matter is accompanied by combustion with the formation of lanthanum dioxycarbonate,  $\text{La}_2\text{O}_2\text{CO}_3$ , or a mixture of  $\text{Ln}_2\text{O}_3$  and  $\text{Ln}_2\text{O}_2\text{CO}_3$  ( $\text{Ln}=\text{Nd}, \text{Sm}, \text{Eu}$ ), however, not in a simple stoichiometric composition. The formation of dioxycarbonate as intermediate was based on the mass losses observed in the TG curves and tests with hydrochloric acid solution on samples heated up to the formation temperature of the intermediate as indicated by the TG curves, confirming the elimination of  $\text{CO}_2$ . The formation of the dioxycarbonate, as intermediate has already been observed for other lanthanides compounds [45, 46]. The last mass loss step is attributed to the thermal decomposition of the dioxycarbonate to the respective  $\text{Ln}_2\text{O}_3$  oxide ( $\text{Ln}=\text{La}, \text{Nd}, \text{Sm}, \text{Eu}$ ). No peak was observed in the DTA curves under the applied experimental settings, which is probably due to the small heat effect of this step.

#### *Cerium(III), Praseodymium(III), Gadolinium(III), Terbium(III) and Dysprosium(III) compounds*

The TG–DTA curves of the cerium(III) and gadolinium(III) as representative of these compounds are

shown in Fig. 3. The first mass loss that occurs up to 120°C (Ce, Pr), 105°C (Gd), 95°C (Tb) and 90°C (Dy) accompanied by an endothermic peak at 105°C (Ce, Pr), 95°C (Gd), 85°C (Tb) and 75°C (Dy) is for the dehydration with loss of 2 (Ce, Pr), 1.5 (Gd); 1 (Tb) and 0.5 (Dy) mole of water, respectively.

The anhydrous compounds are stable up to 260°C (Ce), 320°C (Pr) and 350°C (Gd, Tb, Dy) and the endothermic peak at 250°C (Ce, Pr), 255°C (Gd) and 270°C (Tb, Dy) is ascribed to the reversible crystalline phase transition, which was confirmed by X-ray powder diffraction and TG–DTA curves.

The less thermal stability of the cerium compound is attributed to the oxidation reaction of Ce(III) to Ce(IV) together with the oxidation of the organic matter. This behaviour concerning to the thermal stability of the cerium compound has already been observed for other cerium compounds, too [45, 46].

The thermal decomposition of the anhydrous compounds takes place in two steps. The first one is accompanied by a small exothermic peak for the Gd(III), Tb(III) and Dy(III) and no peak for the Ce(III) and Pr(III) compounds, probably due to the simultaneous thermal decomposition (endothermic) and oxidation of the organic matter (exothermic). The resulting heat in this step is sufficient to produce a small exothermic peak or insufficient to produce a thermal event. The exothermic peak corresponding to the second step is attributed to the oxidation of the organic matter and for the cerium,

**Table 4** Temperature ranges (°C), mass losses (%) and peak temperatures (°C) observed for each step of the TG–DTA curves of the  $\text{Ln}(\text{Bz})_3 \cdot n\text{H}_2\text{O}$  compounds, where  $\text{Ln}$ =yttrium(III) and lanthanides(III),  $\text{Bz}$ =benzoate

Compound		Steps				Crystalline transition
		First	Second	Third	Fourth	
$\text{La}(\text{Bz})_3 \cdot 2\text{H}_2\text{O}$	°C	40–125	320–510	510–555	630–720	
	Loss(%)	6.73	26.67	35.62	4.19	
	Peak (°C)	115 (endo)	470 (exo)	555 (exo)	—	255 (endo)
$\text{Ce}(\text{Bz})_3 \cdot 2\text{H}_2\text{O}$	°C	50–120	260–400	400–510	—	
	Loss(%)	6.70	28.97	32.33	—	
	Peak (°C)	105 (endo)	—	460 (exo)	—	250 (endo)
$\text{Pr}(\text{Bz})_3 \cdot 2\text{H}_2\text{O}$	°C	50–120	320–520	520–560	—	
	Loss(%)	6.84	30.06	31.70	—	
	Peak (°C)	105 (endo)	—	560 (exo)	—	250 (endo)
$\text{Nd}(\text{Bz})_3 \cdot 2.5\text{H}_2\text{O}$	°C	40–120	320–510	510–555	560–680	
	Loss(%)	7.90	32.11	27.29	2.15	
	Peak (°C)	110 (endo)	500 (exo)	555 (exo)	—	250 (endo)
$\text{Sm}(\text{Bz})_3 \cdot 2\text{H}_2\text{O}$	°C	40–110	320–490	490–525	530–680	
	Loss(%)	6.65	32.11	28.29	1.09	
	Peak (°C)	105 (endo)	470 (exo)	525 (exo)	—	230 (endo)
$\text{Eu}(\text{Bz})_3 \cdot 1.5\text{H}_2\text{O}$	°C	40–110	320–470	470–555	555–680	
	Loss(%)	5.15	14.82	46.61	1.07	
	Peak (°C)	100 (endo)	470 (exo)	495, 530 (exo)	—	250 (endo)
$\text{Gd}(\text{Bz})_3 \cdot 1.5\text{H}_2\text{O}$	°C	40–105	350–515	515–550	—	
	Loss(%)	5.03	19.07	42.71	—	
	Peak (°C)	95 (endo)	500 (exo)	550 (exo)	—	255 (endo)
$\text{Tb}(\text{Bz})_3 \cdot \text{H}_2\text{O}$	°C	40–95	350–490	490–530	—	
	Loss(%)	3.40	30.20	31.94	—	
	Peak (°C)	85 (endo)	450 (exo)	530 (exo)	—	270 (endo)
$\text{Dy}(\text{Bz})_3 \cdot 0.5\text{H}_2\text{O}$	°C	40–90	350–500	500–590	—	
	Loss(%)	1.72	22.00	41.28	—	
	Peak (°C)	75 (endo)	450 (exo)	535, 555 (exo)	—	270 (endo)
$\text{Ho}(\text{Bz})_3$	°C	350–535	535–580	—	—	
	Loss(%)	29.46	32.72	—	—	
	Peak (°C)	460 (exo)	565 (exo)	—	—	280 (endo)
$\text{Er}(\text{Bz})_3$	°C	350–545	545–570	—	—	
	Loss(%)	30.24	33.59	—	—	
	Peak (°C)	460 (exo)	570 (exo)	—	—	280 (endo)
$\text{Tm}(\text{Bz})_3$	°C	350–515	515–545	—	—	
	Loss(%)	29.01	34.64	—	—	
	Peak (°C)	460 (exo)	545 (exo)	—	—	280 (endo)
$\text{Yb}(\text{Bz})_3$	°C	350–515	515–550	—	—	
	Loss(%)	36.00	27.34	—	—	
	Peak (°C)	470 (exo)	550 (exo)	—	—	280 (endo)
$\text{Lu}(\text{Bz})_3 \cdot 1.5\text{H}_2\text{O}$	°C	350–535	535–560	—	—	
	Loss(%)	33.44	29.42	—	—	
	Peak (°C)	460 (exo)	560 (exo)	—	—	275 (endo)
$\text{Y}(\text{Bz})_3$	°C	350–530	530–560	—	—	
	Loss(%)	23.68	51.31	—	—	
	Peak (°C)	460 (exo)	560 (exo)	—	—	280 (endo)

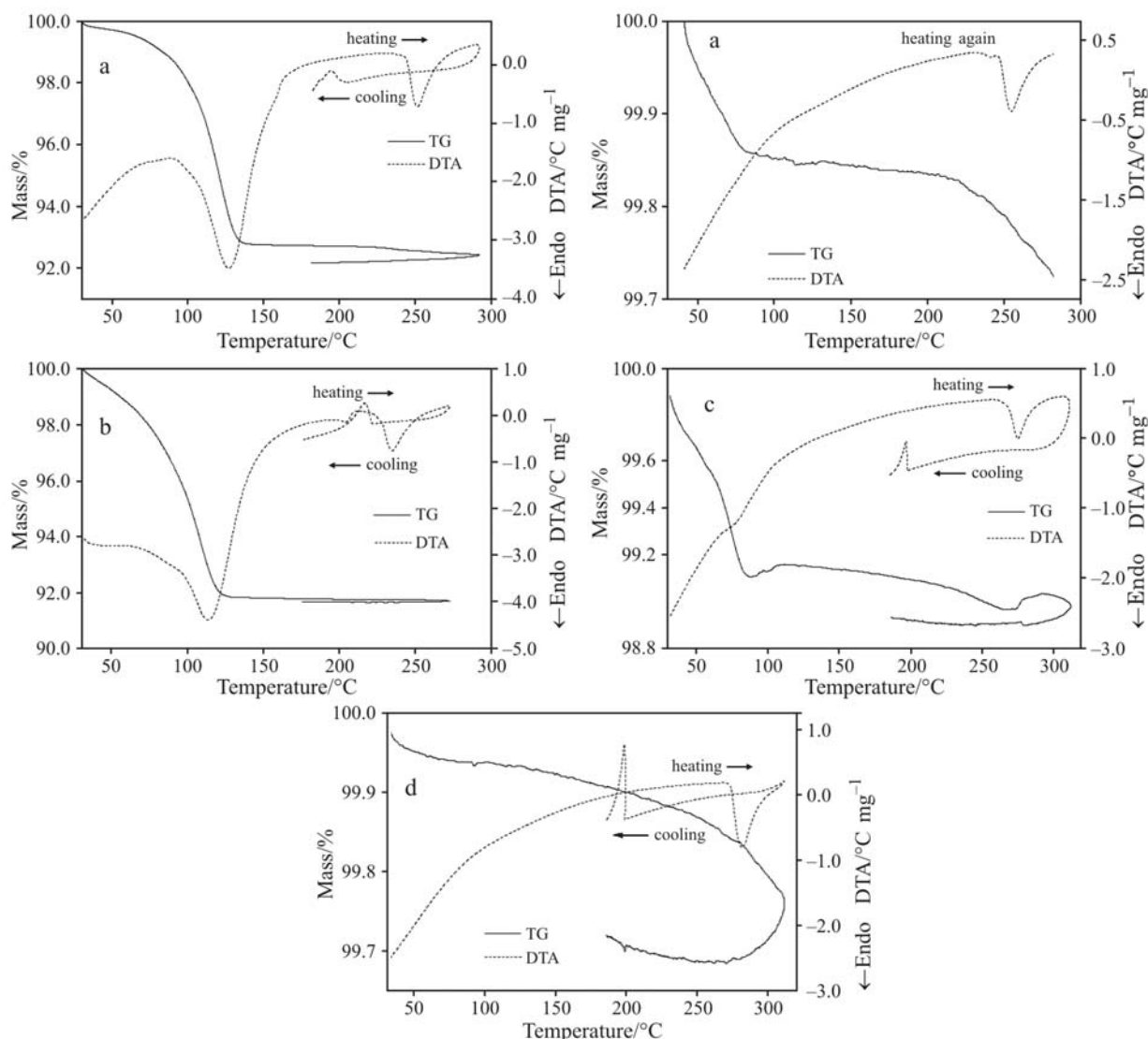


**Fig. 4** TG–DTA curves of: a –  $\text{La}(\text{Bz})_3 \cdot 2\text{H}_2\text{O}$ ; b –  $\text{Sm}(\text{Bz})_3 \cdot 2\text{H}_2\text{O}$ ; c –  $\text{Dy}(\text{Bz})_3 \cdot 0.5\text{H}_2\text{O}$ ; d –  $\text{Yb}(\text{Bz})_3$  ( $\text{Bz}$ =benzoate)

praseodymium and terbium compounds. In this step the oxidation reaction of Ce(III) to Ce(IV), Pr(III) to  $\text{Pr}_6\text{O}_{11}$  and Tb(III) to  $\text{Tb}_4\text{O}_7$ , respectively also occurs. The TG–DTA profiles of this step also show that the oxidation is accompanied by combustion and as final residue the formation of the respective oxide,  $\text{CeO}_2$ ,  $\text{Pr}_6\text{O}_{11}$ ,  $\text{Tb}_4\text{O}_7$ ,  $\text{Gd}_2\text{O}_3$  and  $\text{Dy}_2\text{O}_3$ , without the formation of intermediate,  $\text{Ln}_2\text{O}_2\text{CO}_3$ , as observed for the La(III), Nd(III), Sm(III) and Eu(III) compounds. The lack of the formation of the intermediate is undoubtedly due to the large amount of evolved heat provoked either by the oxidation and combustion of the organic matter (Gd, Dy) together with the oxidation reaction of the lanthanide ions (Ce, Pr, Tb) and yet by a decreasing stability of this intermediate with increasing atomic number of the lanthanide ions [47].

#### Holmium(III) to Lutetium(III) and Yttrium(III) compounds

The TG–DTA curves of the holmium(III) and ytterbium(III) as representative of these compounds are shown in Fig. 3. These curves show that all the compounds were obtained in anhydrous state and they are stable up to 350°C. Above this temperature the anhydrous compounds show mass losses in two steps together with exothermic peaks attributed to the oxidation of the organic matter. The TG–DTA profiles of the last step also show that oxidation of the organic matter is accompanied by combustion and with the formation of the respective oxide,  $\text{Ln}_2\text{O}_3$  ( $\text{Ln}=\text{Ho}$  to Lu and Y) without formation of intermediate, too.

The endothermic peak at 280°C observed in these compounds is attributed to the reversible crystalline phase transition as it can be seen in the

TG–DTA curves (Fig. 4) as representative of the studied compounds.

The mass loss ( $\Delta m$ ), temperature range and peak temperature (°C) observed for each step of the TG–DTA curves of all the compounds were collected in Table 4.

## Conclusions

TG curves and chemical analysis can provide a general formula for these compounds in the solid state.

The X-ray powder patterns showed that all the synthesized compounds exist in crystalline state.

The infrared spectroscopic data suggest that the benzoate acts as a bidentate ligand towards the metal ions considered in this work.

The TG–DTA curves provided information on the thermal stability and thermal behaviour of these compounds.

## Acknowledgements

The authors thank FAPESP, CNPq and CAPES Foundations (Brazil) for financial support and computational facilities of IQ-UNESP and CENAPAD-UNICAMP.

## References

- S. J. Yun, S. K. Kang and S. S. Yun, *Thermochim. Acta*, 331 (1999) 13.
- Z. M. Wang, L. J. Van de Burgt and G. R. Choppin, *Inorg. Chim. Acta*, 293 (1999) 167.
- N. Arnaud and J. Georges, *Analyst*, 125 (2000) 1487.
- G. R. Choppin, P. A. Bertrand, Y. Hasegawa and N. Rizalla, *Inorg. Chem.*, 21 (1982) 3722.
- A. W.-H. Lam, W.-T. Wong, S. Gao, G. Wen and X.-X. Zhang, *J. Inorg. Chem.*, 1 (2003) 149.
- W. W. Wendlandt, *Anal. Chem.*, 17 (1957) 295.
- W. W. Wendlandt, *Anal. Chem.*, 29 (1957) 800.
- A. K. Galwey, *J. Chem. Soc.*, (1965) 6188.
- S. B. Pirkes, G. N. Makushova and A. V. Lapitskaya, *Russ. J. Inorg. Chem.*, 661 (1976) 21.
- S. B. Pirkes, A. V. Lapitskaya and G. N. Makushova, *Russ. J. Inorg. Chem.*, 21 (1976) 816.
- G. N. Makushova, A. V. Lapitskaya, S. O. Goppe and S. B. Pirkes, *Russ. J. Inorg. Chem.*, 24 (1979) 1574.
- S. B. Pirkes, G. N. Makushova, A. V. Lapitskaya and N. P. Tsilina, *Russ. J. Inorg. Chem.*, 28 (1983) 1684.
- W. Lewandowski, *J. Mol. Struct.*, 101 (1983) 93.
- G. N. Makushova and S. B. Pirkes, *Russ. J. Inorg. Chem.*, 29 (1984) 531.
- G. N. Makushova, S. B. Pirkes and E. Yu. Levina, *Russ. J. Inorg. Chem.*, 30 (1985) 652.
- W. Lewandowski and H. Baranska, *J. Raman Spectr.*, 17 (1986) 17.
- G. N. Makushova and S. B. Pirkes, *Russ. J. Inorg. Chem.*, 32 (1987) 489.
- T. Glowiaik, H. Kozlowski, L. Strinna Erre, B. Gulinati, G. Micera, A. Pozzi and S. Brunni, *J. Coord. Chem.*, 25 (1992) 75.
- W. Brzyska and S. Karasinski, *J. Thermal Anal.*, 39 (1993) 429.
- W. Ferenc and B. Bocian, *J. Therm. Anal. Cal.*, 62 (2000) 831.
- B. Bocian, B. Czajka and W. Ferenc, *J. Therm. Anal. Cal.*, 66 (2001) 729.
- B. Czajka, B. Bocian and W. Ferenc, *J. Therm. Anal. Cal.*, 67 (2002) 631.
- W. Ferenc and B. Bocian, *J. Therm. Anal. Cal.*, 74 (2003) 521.
- W. Ferenc and A. Walkow-Dziewulska, *J. Therm. Anal. Cal.*, 71 (2003) 375.
- N. S. Fernandes, M. A. S. Carvalho Filho, C. B. Melios and M. Ionashiro, *J. Therm. Anal. Cal.*, 73 (2003) 307.
- N. S. Fernandes, M. A. S. Carvalho Filho, R. A. Mendes, C. B. Melios and M. Ionashiro, *J. Therm. Anal. Cal.*, 76 (2004) 193.
- W. Ferenc, B. Bocian and A. Walków-Dziewulska, *J. Therm. Anal. Cal.*, 76 (2004) 179.
- E. C. Rodrigues, A. B. Siqueira, E. Y. Ionashiro, G. Bannach and M. Ionashiro, *J. Therm. Anal. Cal.*, 79 (2005) 323.
- A. C. Vallejo, A. B. Siqueira, E. C. Rodrigues, E. Y. Ionashiro, G. Bannach and M. Ionashiro, *Ecl. Quim.*, 30 (2005) 7.
- C. T. Carvalho, A. B. Siqueira, E. C. Rodrigues and M. Ionashiro, *Ecl. Quim.*, 30 (2005) 19.
- E. C. Rodrigues, A. B. Siqueira, E. Y. Ionashiro, G. Bannach and M. Ionashiro, *Ecl. Quim.*, 31 (2006) 21.
- E. C. Rodrigues, A. B. Siqueira, E. Y. Ionashiro, G. Bannach and M. Ionashiro, *Thermochim. Acta*, 451 (2006) 149.
- R. N. Marques, C. B. Melios and M. Ionashiro, *J. Alloys Compd.*, 88 (2002) 344.
- M. Ionashiro, C. A. F. Graner and J. Zuanon Netto, *Ecl. Quim.*, 7 (1985) 10.
- C. C. J. Roothan, *Rev. Mod. Phys.*, 23 (1951) 69.
- T. H. Dunning Jr. and P. J. Hay, *Modern Theoretical Chemistry*, Ed. H. F. Schaefer, New York 1976, pp. 1–28.
- P. J. Hay and W. R. Wadt, *J. Chem. Phys.*, 82 (1985) 270.
- W. R. Wadt and P. J. Hay, *J. Chem. Phys.*, 82 (1985) 284.
- P. J. Hay and W. R. Wadt, *J. Chem. Phys.*, 82 (1985) 299.
- Gaussian 98, Revision A.11.2, M. J. Frisch, G. W. Trucks, H. B. Schlegel, G. E. Scuseria, M. A. Robb, J. R. Cheeseman, V. G. Zakrzewski, J. A. Montgomery, Jr., R. E. Stratmann, J. C. Burant, S. Dapprich, J. M. Millam, A. D. Daniels, K. N. Kudin, M. C. Strain, O. Farkas, J. Tomasi, V. Barone, M. Cossi, R. Cammi, B. Mennucci, C. Pomelli, C. Adamo, S. Clifford, J. Ochterski, G. A. Petersson, P. Y. Ayala, Q. Cui, K. Morokuma, N. Rega, P. Salvador, J. J. Dannenberg, D. K. Malick, A. D. Rabuck, K. Raghavachari, J. B. Foresman, J. Cioslowski, J. V. Ortiz, A. G. Baboul, B. B. Stefanov, G. Liu, A. Liashenko, P. Piskorz, I. Komaromi, R. Gomperts, R. L. Martin, D. J. Fox, T. Keith, M. A. Al-Laham, C. Y. Peng, A. Nanayakkara, M. Challacombe, P. M. W. Gill, B. Johnson, W. Chen,

- M. W. Wong, J. L. Andres, C. Gonzalez,  
M. Head-Gordon, E. S. Replogle, and J. A. Pople,  
Gaussian, Inc., Pittsburgh PA, 2001.
- 41 W. Lewandowski, *J. Mol. Struct.*, 101 (1983) 93.
- 42 W. Lewandowski and H. Baranska, *J. Raman Spect.*,  
17 (1986) 17.
- 43 D. Z. Goodson, *J. Phys. Chem.*, 86 (1998) 659.
- 44 H. B. Schlegel, In new theoretical concepts for understanding organic reaction, J. Berdron, Ed., Academic, The Netherlands 1989, pp 33–53.
- 45 L. C. S. de Oliveira, C. B. Melios, M. Spirandeli Crespi,  
C. A. Ribeiro and M. Ionashiro, *Thermochim. Acta*,  
219 (1993) 215.
- 46 M. H. Miyano, C. B. Melios, C. A. Ribeiro, H. Redigo and  
M. Ionashiro, *Thermochim. Acta*, 221 (1993) 53.
- 47 L. Moscardini D' Assunção, I. Giolito and M. Ionashiro,  
*Thermochim. Acta*, 137 (1989) 319.

---

Received: September 30, 2005

Accepted: March 8, 2007

OnlineFirst: August 31, 2007

---

DOI: 10.1007/s10973-005-7380-6